REFINED ANALYSIS FOR SOIL-PIPE SYSTEMS

Yohchia CHEN, Ph.D., P.E.
Department of Civil Engineering
The Pennsylvania State University
Middletown, PA 17057-4898, U.S.A.

ABSTRACT

This paper discusses a finite element-based refined approach for buried pipes under severe earthquake effects. Modeling and computation techniques using MSC/NASTRAN are described in detail. A number of realistic pipes are investigated. The refined analysis results are compared with those obtained from a simplified method which is the currently accepted method. Special features and advantages of the program are demonstrated. Recommendations for analyzing and designing a buried straight pipe are also made.

INTRODUCTION

For structures such as nuclear power plants, there are many underground safety-related pipes and structural components which are utilized in the operation of the plant. These underground components provide water supply, electrical power, routing of pipes, and movement of personnel to ensure safe operation and safe shutdown of the plant. Examples of these include essential raw cooling water pipes, electrical conduit banks, pipe tunnels and trenches, and personnel tunnels.

Pipes are usually made of steel material, and are long structures supported mostly by the surrounding soils, Fig. 1. Their orientation could vary along the route. However, the scope of the study is limited to buried straight pipes (portion AB, Fig. 1). The underground safety-related pipes and structural components require seismic analysis and design to ensure the safety of nuclear power plants. Generally, this involves layout and qualification of the route, consideration of nonseismic loads that influence layout, determination of seismic loads to be considered, seismic analysis, and seismic design. Furthermore, as a general rule, a simplified method based on the fundamental assumption that pipe deforms the same amount as the surrounding soil is adopted in the practice [1-4]. Though this assumption leads to conservative designs in many situations, its validity and applicability need to be further verified. This paper therefore aims to discuss a more rational analysis method for buried pipes as related to the seismic design. Another emphasis of the paper is to examine the suitability of the design formulas for buried straight pipes.

PROBLEM DESCRIPTION

Fig. 1 shows the typical soil-pipe system where d represents the embedment depth of pipe and D is the outer diameter of pipe. The pipe (ABEFG, Fig. 1) is made of carbon steel, and has total length of 1,050 meters. The outside diameter (D) is 30 inches, and inner diameter is 28.75 inches. The 1940 El Centro earthquake (NS-component), Fig. 2, was chosen as the design earthquake. Based on the measured geological data for the earthquake site (Fig. 3), the soil depth, H (Fig. 1), was set at 34.75 m.

Assumptions for this study include small strain but large displacement problem, flexible pipe, nonliquefied soil, and good bondage between the pipe and the surrounding soil.

BASIC EQUATIONS FOR SIMPLIFIED ANALYSIS FOR BURIED STRAIGHT PIPES

Under the assumption that the pipe moves together with the surrounding soil, the maximum axial strain (ϵ_a) and bending strain (ϵ_b) in a section of a long horizontal pipe (AB, Fig. 1) are conservatively determined by the following equations:

$$\epsilon_a = \pm \frac{v}{V_a} \tag{1}$$

$$\epsilon_b = \pm \frac{R\ a}{V_a^2} \tag{2}$$

where v is the particle velocity, V_a the apparent wave velocity with respect to ground surface, R the outer radius of pipe, and a is the particle acceleration.

Eqns (1) and (2) are simple because material properties are not explicitly involved, but these equations are widely used in practice. For the design earthquake selected (Fig. 2), v= 13.7 in/s, a= 0.34 g (g being the gravity acceleration), and V_a= 2500 ft/s^2. The maximum axial force of straight pipe, P_1, is simply calculated from [1, 5, 6]:

$$P_1 = A\ E_p\ \epsilon_a \tag{3}$$

where A is the cross-sectional area of pipe, and E_p is the Young's modulus of pipe.

According to the empirical relationship of Sakurai and Takahashi [1], P_1 is limited to:

$$P_{max} = 0.25\ F\ L \tag{4}$$

where F is the friction force per unit length of pipe, and L is the wave length of seismic waves which can be found from

$$L = T_0\ c \tag{5}$$

where T_0 is the predominant period of seismic waves which can be determined from a site specific analysis.

"F" in eqn (4) is smaller of

$$F = f\ \sigma\ \pi\ D \tag{6}$$

and

$$F = \tau\ \pi\ D \tag{7}$$

where f is the friction coefficient (= 0.5 approximately), σ the average effective vertical stresses (or the average overburden pressure) of the soil surrounding the pipe, D is the outer diameter of pipe, and τ is the shear stress defined by the Mohr-Coulomb law:

$$\tau = c + \sigma \tan \phi \tag{8}$$

where c is the soil cohesion, and ϕ is the internal friction angle of soil particles.

The maximum bending moment of straight pipe, M_1, on the other

hand, can be computed from [1, 5, 6]:

$$M_1 = S\ E_p\ \epsilon_b \tag{9}$$

where S is the section modulus of pipe.

"σ" in eqns (6) and (8) depends upon the embedment depth of pipe (d, Fig. 1), pipe diameter (D) and the unit weight of soil. In practice, homogeneous and dry soil throughout the entire soil depth (H, Fig. 1) is usually assumed to calculate σ and τ. Namely, <u>average</u> soil properties (Young's modulus, Poisson's ratio, unit weight, c, and ϕ) are often used. In reality, soil stratum is layered with various material properties, and the ground water table fluctuates seasonally.

GOVERNING EQUATION FOR THE REFINED ANALYSIS

For linear analyses, the modal approach using the finite element method was employed. This is an effective method because in seismic response analysis only a few mode shapes are needed and the physical system is only locally nonlinear. While for nonlinear analyses, the direct nonlinear transient approach was used. The nonlinear finite element equilibrium equations for the solution of the response at time t+Δt are

$$[M]\ \{\ddot{U}\}^{(i)} + [C]\ \{\dot{U}\}^{(i)} + [K]_\tau\ \{\Delta U\}^{(i)} = \{R\} - \{F\}^{(i-1)} \quad (i=1, 2, \ldots) \tag{10}$$

where [M] is the mass matrix, [C] the damping matrix, $[K]_\tau$ the stiffness matrix corresponding to the configuration at some previous time τ, $\{\ddot{U}\}$ the acceleration vector, $\{\dot{U}\}$ the velocity vector, $\{\Delta U\}$ the displacement vector, {R} the externally applied load vector, and {F} is the nodal force vector.

Upon solving Equation (10), an integration scheme based on the Newmark method [7] and the subspace iteration method for nonlinear analyses [8] were used.

As mentioned above, modal formulation is adopted for linear analyses. Since for a structural vibration problem damping is proportional to stiffness and mass, the mode shape vectors decouple. The displacements at time t+Δt, $\{U\}_{t+\Delta t}$, can therefore be determined from

$$\{U\}_{t+\Delta t} = \sum_{i=r}^{s} \{\phi\}_i\ x_{i,t+\Delta t} \tag{11}$$

where r and s are the two distinct numbers of mode shapes, $\{\phi\}_i$ the eigen vector for ith mode, and $x_{i,t+\Delta t}$ is the ith generalized modal displacement at time t+Δt.

Decoupling of eqn (10) is achieved through the use of eqn (11) and the following transformation

$$[K]_\tau \{\phi\}_i = \omega_i^2 [M] \{\phi\}_i \qquad (i= r,\ldots., s) \tag{12}$$

where ω_i and $\{\phi\}_i$ are the frequency and mode shape vector of free vibration system at time τ, respectively.

The decoupled form of eqn (10) at time t+Δt therefore becomes

$$\{\ddot{X}\}^{(i)} + [\Omega_1] \{\dot{X}\}^{(i)} + [\Omega_2] \{\Delta X\}^{(i)}$$

$$= [\Phi]^T (\{R\} - \{F\}^{(i-1)}) \qquad (i= 1, 2, \ldots) \tag{13}$$

where $\{\ddot{X}\}$ is the generalized acceleration vector, $\{\dot{X}\}$ the generalized velocity vector, $\{\Delta X\}$ the generalized displacement vector, $[\Omega_1]$ a diagonal matrix consisting of $2\,\xi_r\,\omega_r, \ldots, 2\,\xi_s\,\omega_s$ (ξ = damping ratio), $[\Omega_2]$ a diagonal matrix consisting of $\omega_r^2, \ldots, \omega_s^2$, and $[\Phi]$ is a matrix consisting of mode shape vectors $\{\phi\}_r, \ldots, \{\phi\}_s$.

The generalized (internal) forces (forces, moments) at time t+Δt, $\{P\}_{t+\Delta t}$, involving in the system can then be computed from the force-displacement relation

$$\{P\}_{t+\Delta t} = [K]_\tau \{X\}_{t+\Delta t} \tag{14}$$

It should be noted here that linear analysis should always precede a nonlinear analysis as a good practice.

NUMERICAL MODELING

Since the main interest of this study was the buried pipe itself, the large permanent structures, pumping station and reactor building, were simply modeled as concentrated structural masses. The pipe system (ABEFG) was assumed to be completely fixed at A and G, Fig. 1. To account for flexibility and material nonlinearity, the pipe was represented by isoparametric beam/pipe elements. While the soil was represented by four-node TETRA elements with aspect ratio (element length/element width) of four or less.

Concentrated dampers representing the special nontransmitting boundary conditions were imposed at the nodes along the lateral boundaries for eliminating the spurious wave reflections from the finite model [9]. To facilitate the computation, the structure (pipe) was separated from the soil. The structure and soil are linked by the interface nodes. This substructuring technique is especially effective for a nonlinear seismic analysis [10, 11].

Damping ratios (ξ) were 3 percent (structure) and 7 percent (soil) for the linear analysis, and 6 percent (structure) and 11 percent (soil) for the nonlinear analysis.

For nonlinear analysis, a plasticity model with nonassociated flow rule based on the one proposed by DiMaggio and Sandler [12] was used for soil. This model is proven to be very effective for a dynamic soil-structure interaction problem [13]. For steel material, an elastic-plastic model with isotropic hardening was used. To obtain better results and study the interface behavior, a

special material model is needed for the interface. In this study, the no-tension model with thin-layer concept discussed in references [14] and [15] was utilized.

The first ten-second ground accelerations of the design earthquake (Fig. 2) were applied at the bottom of soil-pipe system. Two computer programs, ADINA [16] and MSC/NASTRAN [17], were employed for verification and quality control checks. Typical finite element mesh is shown in Fig. 4. The total computation time using MSC/NASTRAN [17] in IBM3090s mainframe machine was approximately 1½ minutes for a typical linear analysis, and 42 minutes for a nonlinear modal analysis. Computation time was slightly less using ADINA [16].

NUMERICAL EXAMPLES AND RESULTS

The numerical studies covered three typical burial conditions for the horizontal pipe (AB, Fig. 1): shallowly-buried pipes ($d/D \leq 4$), moderately-buried pipes ($4 \leq d/D \leq 8$), and deeply-buried pipes ($8 \leq d/D \leq 12$); two soil conditions (uniform soil, layered soil); two extreme ground water table conditions (low water table, high water table); and two types of analysis (linear, nonlinear). The low water table condition means that the ground water table is below the bottom of the soil-pipe system. While the high water table condition means that the ground water table is on the ground level.

The steel pipe has yielding stress of 36 ksi. The elastic soil properties used in this study are summarized in Table 1 in which the weight of layer thickness was considered in determining the average soil properties for the uniform soil condition. Tables 2-5 summarize and compare the maximum earthquake forces (axial load, and bending moment) obtained from the linear analyses for the straight pipes. Nonlinear analysis results are contained in Table 6.

DISCUSSION

Based on the obtained results, the following noticeable points were found for the horizontally buried straight pipes:

1. For pipes with **$d/D < 1$** (relatively shallow pipes), the simplified method using eqn (3) undesirably underestimated the maximum axial force of the pipe, particularly when the ground water table is high (see Tables 2 and 4). While for pipes with $d/D \geq 1$, the maximum earthquake forces (axial forces, P_1, and bending moments, M_1) were governed by the characteristics of earthquake ground motion using the simplified method [eqns (3) and (9)]. Namely, for majority of the pipes the simplified method apparently did not consider the variation of geological conditions (soil

properties, ground water table), Tables 2-5.

2. The simplified method generally produced higher earthquake forces than the refined method (Tables 2-6). The conservatism of the simplified method is amplified as the pipe embedment is increased (variation as large as 45 percent being observed in Table 2).

3. As shown in Tables 2-6, the refined method displayed the effects from soil layering and ground water table fluctuation. P_1 and M_1 of the layered soil condition were about 10 percent higher than those of the uniform soil condition. As compared to the low water table condition, the high water table condition resulted in higher P_1 values (8-14 percent, Tables 2 and 4) and higher M_1 values (5-11 percent, Tables 3 and 5).

4. The nonlinear results (Table 6) were lower by about 22 percent than the linear ones (Tables 2-5).

5. The MSC/NASTRAN's results compared fairly well with the ADINA's, Tables 2-5.

CONCLUSIONS AND RECOMMENDATIONS

The current simplified method of predicting the maximum earthquake forces for horizontally buried straight pipes does not consider the dynamic soil-structure interaction, and is therefore too conservative for deeply-buried pipes. Also, it does not consider the embedment of pipe and the variation of geological conditions as arising from soil layering and ground water table fluctuation. The finite element based refined method is capable of handling a general soil-pipe system with the consideration of dynamic soil-structure interaction and nonlinearities. Overall, the computer program MSC/NASTRAN [17] is better mainly because of the wider availability of elements and material models, and hence it results in higher accuracy of computational results. The issue of accuracy becomes more important for more complex pipe problems, such as bent pipes (e.g. near joint B, Fig. 1).

Nevertheless, the simple equations for estimating maximum earthquake-induced forces, like eqns (3) and (9), are desirable from practical viewpoint. To account for the important system parameters discussed, the present form of the simple formulas may be modified by including soil material factors (f_1), water table factors (f_2) and embedment factors (f_3). The new form of eqn(3) will then appear as $P_1 = f_1\ f_2\ f_3\ A\ E_p\ \epsilon_a$, for example.
These modification factors (f_1-f_4) can be determined from the parametric studies using the refined method.

REFERENCES

1. Sakurai, A., and Takahashi, T., "Dynamic Stresses of Underground Pipe Lines during Earthquakes," In Proc. 4th World Conf. Earthq. Eng., Santiago, Chile, 1969.

2. Nasu, M., Kazama, S., Morioka, T., and Tamura, T., "Vibration Test of the Underground Pipe with a Comparatively Large Cross Section," In Proc. 5th World Conf. Earthq. Eng., 1974.

3. Tamura, C., "Design of Underground Structures by Considering Ground Displacement during Earthquakes," In Proc. US/Japan Seminar Earthq. Eng. Research: Lifeline Sys., Tokyo, Japan, 1976.

4. Nakayama, S., Kiyomiya, O., and Tsuchida, H., "Observation of Dynamic Behavior of Kinuura Submerged Tunnel during Earthquakes," In Proc. 9th Joint Mtg. US/Japan Wind & Seismic Effects, Tokyo, Japan, 1977.

5. Goodling, E. C., "Flexibility Analysis of Buried Pipe," In Proc. ASME/CSME PVP Conf., Montreal, Canada, 1978.

6. Goodling, E. C., "More on Flexibility Analysis of Buried Pipe," In Proc. ASME PVP Conf., San Francisco, CA, 1980.

7. Newmark, N. M., "A Method of Computation for Structural Dynamics," J. Eng. Mech., ASCE, Vol. 85, pp. 67-94, 1959.

8. Bathe, K. J., and Wilson, E. L., Numerical Methods in Finite Element Analysis, Sect. 12.3, Prentice-Hall, Englewood Cliffs, NJ, 1976.

9. Chen, Y., and Krauthammer, T., "Seismic Effects on Large RC Lifelines: I. Theory," Comput. & Struct., Vol. 42, No. 2, pp. 129-135, 1993.

10. Bathe, K. J., and Gracewski, S., "On Nonlinear Dynamic Analysis Using Substructuring and Mode Superposition," Comput. & Struct., Vol. 13, pp. 699-707, 1981.

11. Chen, Y., and Krauthammer, T., "A Combined ADINA-Finite Difference Approach with Substructuring for Seismically Induced Nonlinear Soil-Structure Interaction Problems," Comput. & Struct., Vol. 32, No. 3/4, pp. 779-785, 1989.

12. DiMaggio F. L., and Sandler, I. S., "Material Model for Granular Soils," J. Eng. Mech., ASCE, Vol. 97, No. EM3, pp. 935-950, 1971.

13. Krauthammer, T., and Chen, Y., "Dynamic Soil-Structure Interaction of Rectangular Reinforced Concrete Lifelines," J.

Eng. Struct., Vol. 8, pp. 181-190, 1986.

14. Chen, Y., and Krauthammer, T., "Soil-Structure Interface Effects on Dynamic Interaction Analysis of Reinforced Concrete Lifelines," Soil Dyn. & Earthq. Eng., Vol. 8, No. 1, pp. 32-42, 1989.

15. Chen, Y., "Interface Effects of Box-Type Reinforced Concrete Structures: I. Theory," Comput. & Struct., Vol. 47, No. 3, pp. 383-390, 1993.

16. ADINA, A General Computer Program- Automatic Dynamic Incremental Nonlinear Analysis, Report ARD 90-4 (Users Manual), ADINA R&D, Inc., Watertown, MA, 1990.

17. MSC/NASTRAN, User's Manual. Version 66A, The MacNeal-Schwendler Corp., Los Angeles, CA, 1989.

APPENDIX I. CONVERSION OF UNITS

1 in = 2.54 cm ; 1 ft = 0.3048 m

1 ft/s = 0.3048 m/s

1 lb = 4.45 N ; 1 lb-in = 0.113 N-m

1 lb/in^2 (psi) = 6900 N/m^2 (Pa) ; 1 kPa = 1,000 Pa

1 lb/ft^3 = 16.03 kg/m^3 = 0.01603 t/m^3

Table 1. Soil properties

Soil Layer	thickness (m)	Young's Modulus (kPa)	Possion's Ratio		cohesion (kPa)	Internal Friction Angle (deg)	Unit Weight (kg/m)	
			dry	sat.			moist	sat.
1	4.89	27600	0.36	0.45	120	30	1918	1998
2	16.64	41400	0.36	0.45	192	30	1918	2078
3	13.22	144900	0.33	0.40	4.8	40	1950	2158
Avg.		78823	0.35	0.43	110	34	1934	2094

Note: Avg.= (weighted) average; sat.= saturated

Table 2. Maximum axial forces of the pipes (P_1)
(Low Water Table; Linear Analysis)

(units: lbs)

d/D	Simplified Analysis		Finite Element Analysis			
			uniform soil		layered soil	
	uniform soil	layered soil	ADINA	MSC/NASTRAN	ADINA	MSC/NASTRAN
0	196748	195122	378288	383659	404019	409756
1	446269	446269	365217	370403	302878	307179
2	446269	446269	356417	361478	382820	388254
3	446269	446269	352017	357015	378420	383791
4	446269	446269	347617	352553	374019	379329
5	446269	446269	343217	348090	369618	374866
6	446269	446269	338816	343627	365218	370403
7	446269	446269	330016	334702	356417	361478
8	446269	446269	321215	325776	343220	348090
9	446269	446269	303615	307926	325617	330239
10	446269	446269	286014	290075	303615	307926
11	446269	446269	259613	263299	281614	285612
12	446269	446269	242012	245448	268415	272224

Table 3. Maximum bending moments of the pipes (M_1)
(Low Water Table; Linear Analysis)

(units: lb-in)

d/D	Simplified Analysis		Finite Element Analysis			
	uniform soil	layered soil	uniform soil		layered soil	
			ADINA	MSC/NASTRAN	ADINA	MSC/NASTRAN
0	15652	15652	13426	13617	14045	14243
1	15652	15652	13120	13304	13890	14087
2	15652	15652	12965	13148	13814	14009
3	15652	15652	12808	12991	13580	13774
4	15652	15652	12655	12835	13350	13539
5	15652	15652	12348	12522	13273	13461
6	15652	15652	12192	12365	13118	13304
7	15652	15652	11880	12052	12810	12991
8	15652	15652	11730	11896	12500	12678
9	15652	15652	11420	11582	11806	11974
10	15652	15652	10960	11113	11420	11582
11	15652	15652	10342	10487	10804	10956
12	15652	15652	9260	9391	10032	10174

Table 4. Maximum axial forces of the pipes (P_1)
(High Water Table; Linear Analysis)

(units: lbs)

d/D	Simplified Analysis		Finite Element Analysis			
			uniform soil		layered soil	
	uniform soil	layered soil	ADINA	MSC/NASTRAN	ADINA	MSC/NASTRAN
0	111545	101789	423436	429448	446620	452961
1	334635	305366	409138	414947	436582	442781
2	446269	446269	404820	410567	418022	423956
3	446269	446269	496019	401642	413620	419493
4	446269	446269	387220	392717	411421	417263
5	446269	446269	382816	388294	409222	415030
6	446269	446269	378418	383791	404818	410567
7	446269	446269	369619	374866	391617	397179
8	446269	446269	360820	365941	382818	388254
9	446269	446269	352016	357015	365216	370403
10	446269	446269	321215	325776	338816	343627
11	446269	446269	294814	299000	316814	321314
12	446269	446269	268414	272224	294815	299000

Table 5. Maximum bending moments of the pipes (M_1)
(High Water Table; Linear Analysis)

(units: lb-in)

d/D	Simplified Analysis		Finite Element Analysis			
			uniform soil		layered soil	
	uniform soil	layered soil	ADINA	MSC/NASTRAN	ADINA	MSC/NASTRAN
0	15652	15652	14198	14400	14969	15182
1	15652	15652	14120	14322	14815	15026
2	15652	15652	13965	14165	14660	14869
3	15652	15652	13890	14087	14582	14791
4	15652	15652	13735	13930	14506	14713
5	15652	15652	13580	13774	14352	14556
6	15652	15652	13274	13461	14199	14400
7	15652	15652	13119	13304	13890	14087
8	15652	15652	12964	13148	13582	13774
9	15652	15652	12655	12835	13274	13461
10	15652	15652	12459	12635	12501	12678
11	15652	15652	11266	11426	11883	12052
12	15652	15652	9877	10017	10650	10800

Table 6. Maximum earthquake forces for straight pipes (P_1, M_1)
(Nonlinear Analysis by MSC/NASTRAN)

(unit: lbs for P_1 and lb-in for M_1)

	Axial Force				Bending Moment			
	L.W.T.		H.W.T.		L.W.T.		H.W.T.	
d/D	uniform soil	layered soil	uniform soil	layered soil	uniform soil	layered soil	uniform	layered
0	300405	320839	336258	354669	10662	11153	11275	11888
1	290026	310991	324904	346697	10417	11030	11214	11765
2	283037	304003	321474	331957	10295	10969	11091	11643
3	279543	300509	314486	328463	10172	10785	11030	11581
4	276049	297014	307497	326716	10050	10601	10907	11520
5	272554	293520	304003	324969	9804	10540	10785	11398
6	269060	290026	300509	321474	9682	10417	10540	11275
7	262071	283037	293520	310991	9437	10172	10417	11030
8	255083	272554	286531	304003	9314	9927	10295	10785
9	241106	258577	279543	290026	9069	9375	10050	10540
10	227129	241106	255083	269060	8701	9069	9682	9927
11	206163	223634	234117	251589	8211	8579	8947	9437
12	192186	213151	213151	234117	7353	7966	7844	8456

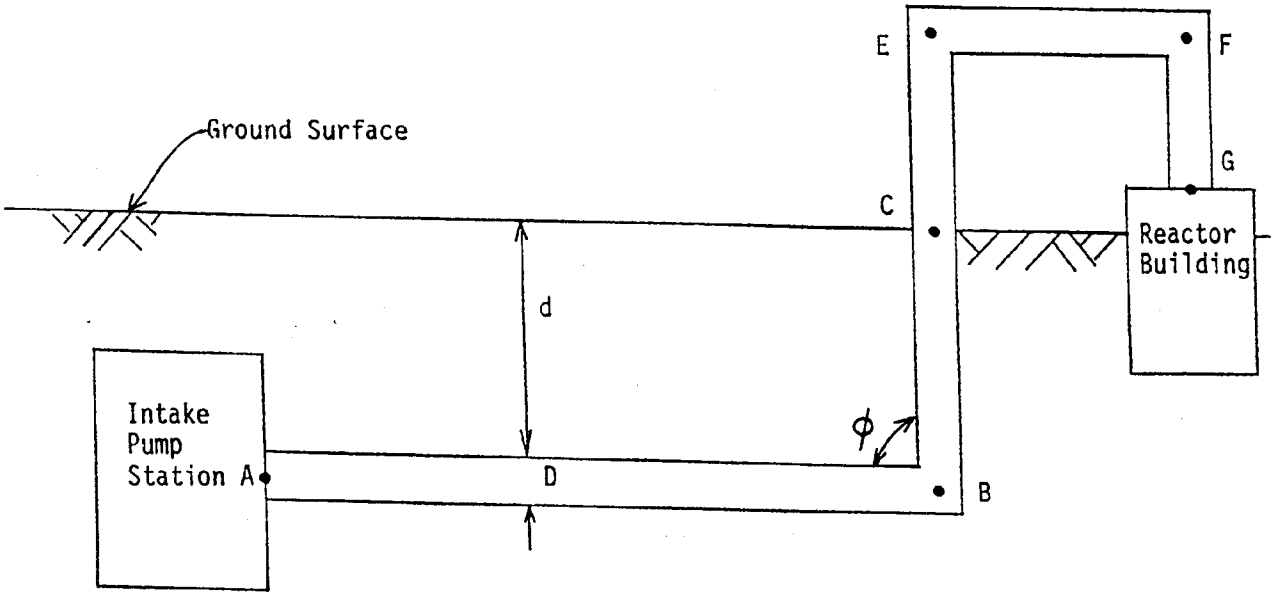

(AB= 600 m, BE= 300 m, EF= 120 m, FG= 30 m)

Figure 1. Typical soil-pipe system.

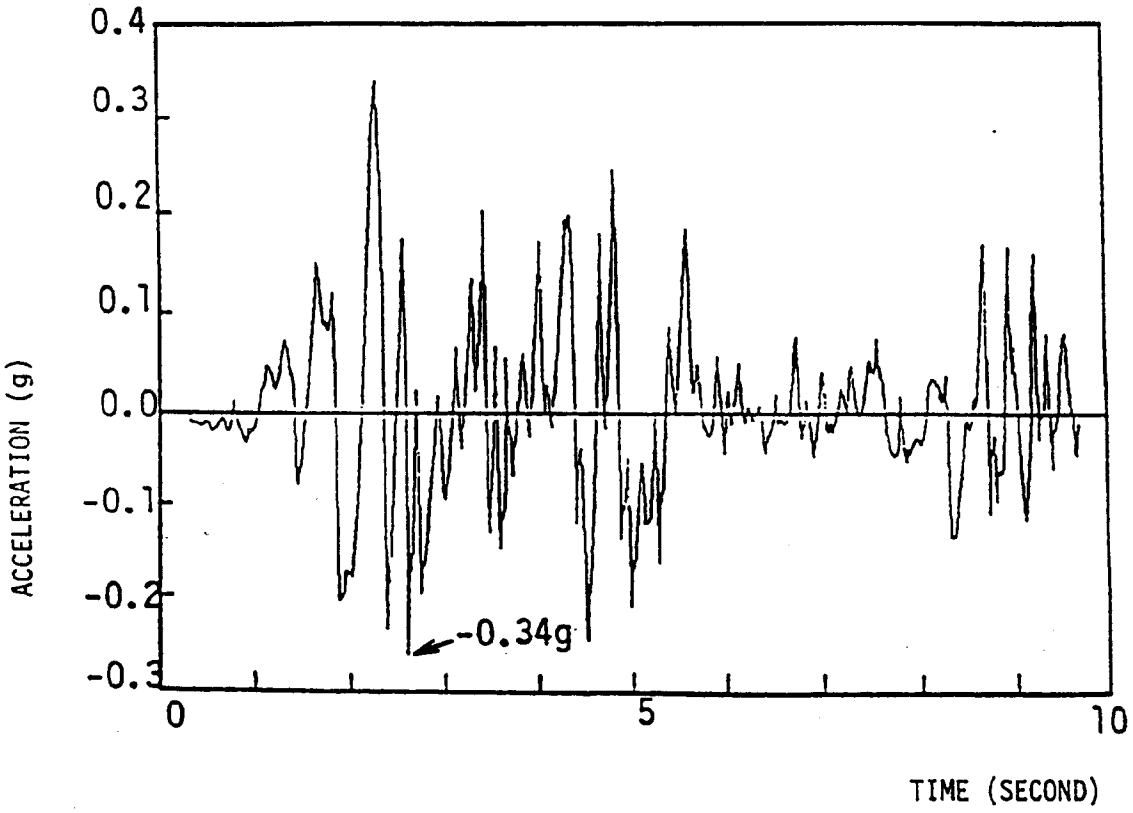

FIGURE 2. The ground accelerations of the 1940 El Centro earthquake (NS-component).

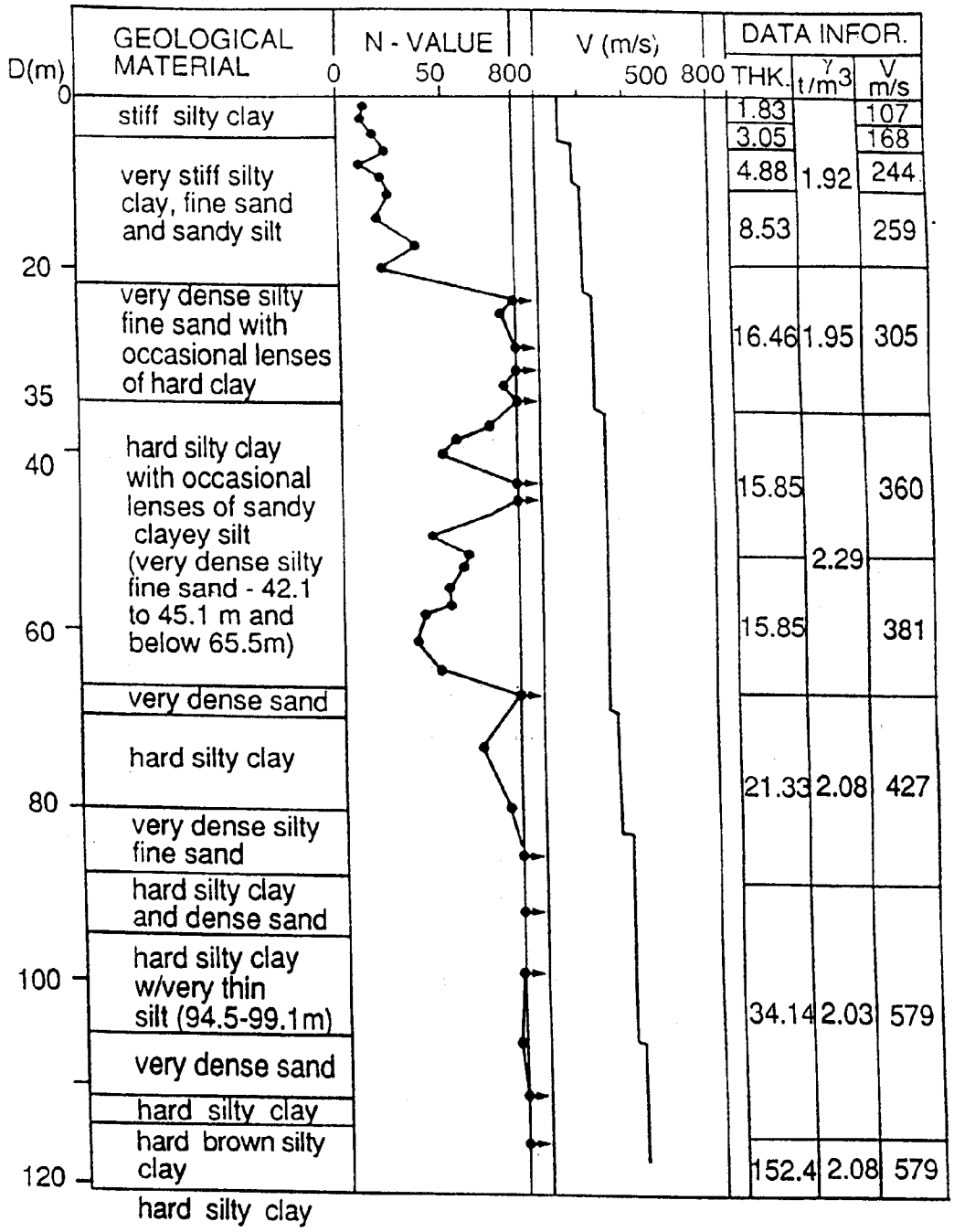

FIGURE 3. The geological data measured at the earthquake site.

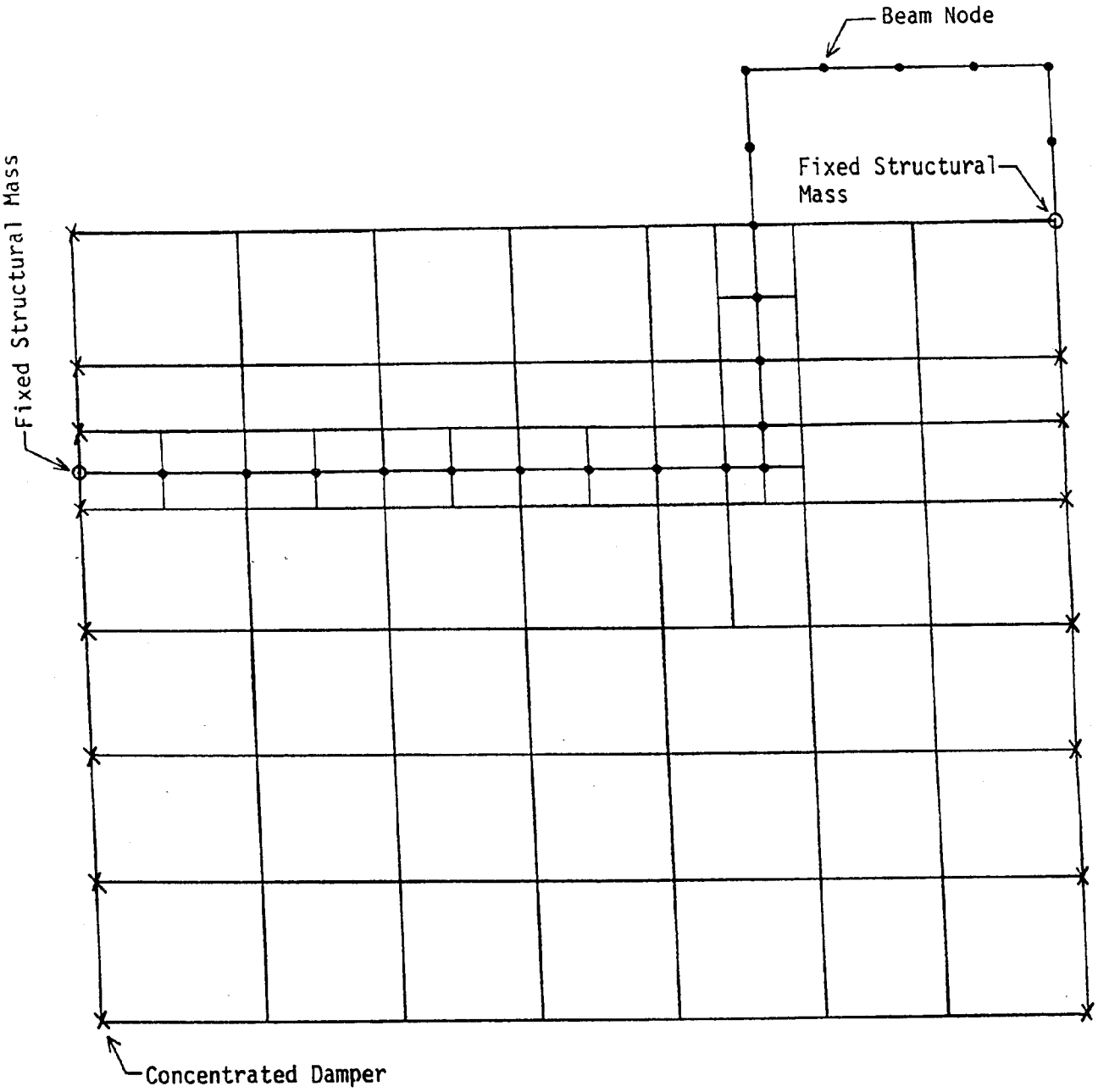

Figure 4. Typical finite element mesh (22 beam elements; 28 interface elements; 45 soil elements).